Neural latencies across auditory cortex of macaque support a dorsal stream supramodal timing advantage in primates

Corrie R. Camalier[a,b,1], William R. D'Angelo[a], Susanne J. Sterbing-D'Angelo[a], Lisa A. de la Mothe[c,d], and Troy A. Hackett[a,c]

[a]Department of Psychology, Vanderbilt University, Nashville, TN 37240; [b]Department of Neurological Surgery and [c]Department of Hearing and Speech Sciences, Vanderbilt University School of Medicine, Nashville, TN 37232; and [d]Department of Psychology, Tennessee State University, Nashville, TN 37209

Edited* by Mortimer Mishkin, National Institute for Mental Health, Bethesda, MD, and approved September 26, 2012 (received for review April 16, 2012)

Sensory systems across the brain are specialized for their input, yet some principles of neural organization are conserved across modalities. The pattern of anatomical connections from the primate auditory cortex to the temporal, parietal, and prefrontal lobes suggests a possible division into dorsal and ventral auditory processing streams, with the dorsal stream originating from more caudal areas of the auditory cortex, and the ventral stream originating from more rostral areas. These streams are hypothesized to be analogous to the well-established dorsal and ventral streams of visual processing. In the visual system, the dorsal processing stream shows substantially faster neural response latencies than does the ventral stream. However, the relative timing of putative dorsal and ventral stream processing has yet to be explored in other sensory modalities. Here, we compare distributions of neural response latencies from 10 different areas of macaque auditory cortex, confirmed by individual anatomical reconstructions, to determine whether a similar timing advantage is found for the hypothesized dorsal auditory stream. Across three varieties of auditory stimuli (clicks, noise, and pure tones), we find that latencies increase with hierarchical level, as predicted by anatomical connectivity. Critically, we also find a pronounced timing differential along the caudal-to-rostral axis within the same hierarchical level, with caudal (dorsal stream) latencies being faster than rostral (ventral stream) latencies. This observed timing differential mirrors that found for the dorsal stream of the visual system, suggestive of a common timing advantage for the dorsal stream across sensory modalities.

systems neuroscience | neurophysiology | hierarchy

An enduring question of brain organization is whether some design principles are conserved across sensory systems. Although sensory systems are clearly highly specialized for the particular inputs emitted by their peripheral receptors, might there exist common schemas by which these circuits abstract and process sensory information? One such schema thought to be shared across modalities is the principle of spatial locality, which can be invoked to account for the existence of processing modules and topographic maps (1, 2). However, the brain is a dynamic system: are there principles of temporal organization that are also conserved? Thirty years ago, based on lesion studies and supported by anatomical connections, it was proposed that the visual system could be divided into dorsal and ventral streams (3, 4), hypothesized to correspond to visual spatial and visual object processing, respectively (i.e., "what" vs. "where"). Later investigations showed that neural onset latencies are faster in areas within the dorsal stream (5, 6); thus, the dorsal stream exhibits a significant timing advantage over the ventral stream.

Are other sensory modalities organized into dual processing streams as well? There is emerging evidence that in the auditory system, the projections of auditory cortex to areas in the prefrontal and limbic cortices are organized similarly to the dorsal and ventral streams of the visual system (7–9) (Fig. 1). The dorsal stream originates in the caudal portion of auditory cortex and the ventral stream originates in the rostral portion of auditory cortex. Possible functional homologies between the dual visual and dual auditory streams remain an active area of investigation. In seeking to discover common organizational principles of the brain, it is natural to ask whether the putative dorsal stream of the auditory system also exhibits a timing advantage over the ventral auditory stream.

Current models propose that the primate auditory cortex contains three regions: core, belt, and parabelt (Fig. 2). These three broad regions, which likely comprise distinct functional levels of processing, can be subdivided into approximately 13 different areas, each distinguished by a unique anatomical profile (10, 11). Although detailed studies of connections are lacking, known connectivity patterns suggest the presence of both serial and parallel processing in the auditory cortex: information flows serially from core to belt to parabelt, but appears to be processed in parallel within a region [i.e., within core: A1 (auditory area 1), R (rostral), RT (rostrotemporal)]. The parabelt region, for example, receives inputs from the belt but not the core (12), suggesting that information processing between regions proceeds serially from core to belt to parabelt. In contrast, the auditory cortex receives multiple parallel streams of input from the thalamic medial geniculate complex (MGC). Thalamic input to cortical core areas mainly comes from the ventral division (MGv), input to cortical belt and parabelt areas comes from the anterior and posterior subdivisions of the dorsal division (MGad and MGpd), and all three regions receive input from the medial division (MGm) (13–15).

What timing of cortical activation would be predicted based on known patterns of connectivity in the auditory cortex? Serial cortical connections imply an interregional flow from core to belt to parabelt, leading to the prediction that the latencies of parabelt neurons should be longer than those of core neurons. Corticocortical laminar projection patterns appear to favor a caudal-to-rostral feedforward pattern between areas within a region (reviewed in ref. 11; 16–18,). Thus, these patterns suggest that within a single region, neurons in caudal areas should have faster latencies than single in rostral areas.

Consistent with these predictions, a comparison of latencies between core A1 and lateral belt ML (middle lateral) reported longer neural response latencies in belt than core (19). In the medial belt areas CM (caudomedial), MM (middle medial), and RM (rostromedial), however, latencies have been found to be the same or shorter than in the adjoining core (19–22, but see also ref. 23). Belt latencies that are the same or faster than the

Author contributions: C.R.C., W.R.D., S.J.S.-D., and T.A.H. designed research; C.R.C., L.A.d.l.M., and T.A.H. performed research; C.R.C., L.A.d.l.M., and T.A.H. analyzed data; and C.R.C. and T.A.H. wrote the paper.

The authors declare no conflict of interest.

*This Direct Submission article had a prearranged editor.

[1]To whom correspondence may be addressed. E-mail: corrie.camalier@vanderbilt.edu.

This article contains supporting information online at www.pnas.org/lookup/suppl/doi:10.1073/pnas.1206387109/-/DCSupplemental.

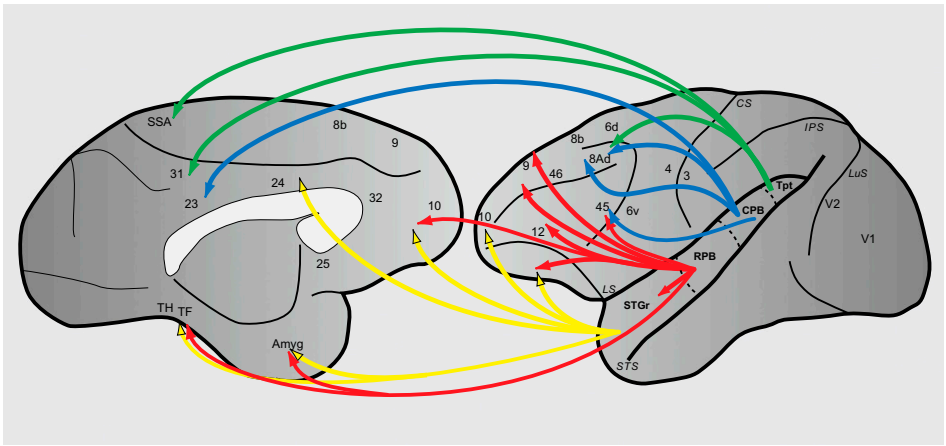

Fig. 1. Auditory cortical projections to prefrontal, limbic structures to show dorsal and ventral streams. Schematic of long-range connections of auditory and auditory-related cortical fields to prefrontal and limbic structures projected on a macaque brain. Note the topography of streams to prefrontal cortex, with dorsal streams in green and blue and ventral streams are in yellow and red. For simplicity, projections from core and belt are excluded.

core pose a problem for the serial flow model, and suggest that parallel inputs arising outside of A1 (such as from thalamus, discussed below) may be contributing to this short latency activity in portions of the belt (20, 21). Intriguingly, there is also increasing evidence that latencies increase within a region in a caudal-to-rostral direction, both in the core and in medial belt (22–26), despite the absence of connectivity to directly support this. Although the available evidence is intriguing, differences in species, stimuli, methods, and anesthetic state between studies make meaningful cross-area and cross-region comparisons difficult to draw. Many areas of the primate auditory cortex have not been characterized physiologically [in particular, parabelt areas CPB (caudal parabelt) and RPB (rostral parabelt)] because of difficulty of access in the macaque, which makes precise areal reconstruction difficult.

This study aims to cohesively examine response latencies of neurons across multiple areas in the same species and under the same conditions. Specifically, we aim to evaluate whether latencies increase along the proposed core-belt-parabelt processing hierarchy as predicted by anatomical connections, as well as whether latencies increase within a region in a caudal-to-rostral direction, as suggested by preliminary physiological evidence. In this study, we compare distributions of response latencies from 10 different areas covering all three regions of the macaque auditory cortex. For click, noise, and tone stimuli, latencies increase mediolaterally within the regional level, but increase even more strongly along the caudal-to-rostral axis within a region. The auditory dorsal stream originates from caudal areas. Taking these data together, this suggests that the dorsal stream of the auditory system is faster than the ventral stream, a schema strikingly similar to the timing advantage seen in the dorsal stream of the cortical visual system.

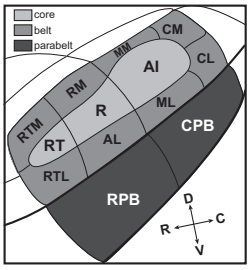

Fig. 2. Schematic of primate auditory cortex (left hemisphere). Overlying parietal cortex is cut off and auditory cortex is partially flattened to reveal organization. The three areas that constitute the core region (A1, R, RT) are in light gray, the eight areas that constitute the belt region (CM, MM, RM, RTM, CL, ML, AL, RTL) are in medium gray, and the two areas that constitute the parabelt (CPB, RPB) are in dark gray. Arrows at the bottom right indicate rostro-caudal and dorso-ventral directions.

Results

Cortical Areas, Neural Onset Latency, Design. Overall 1,656, 1,335, and 1,583 units across the primate auditory cortex were analyzed for click, noise, and tone responses, respectively, using the Gaussian SD method (see *Methods*). These neurons were distributed across 10 areas representing the three regions of auditory cortex [core areas A1 and R, belt areas CM, CL (caudolateral), RM, MM, AL (anterolateral), ML, and parabelt areas CPB and RPB; see *SI Text* for reconstruction detail]. Areas and number of neurons recorded and analyzed are reported in Table 1. The rostral-most areas RTM (rostrotemporal medial), RT, and RTL (rostrotemporal lateral) were not well-covered by the recording grid, and therefore were not included. In addition, the grid also did not allow access to the rostral tip of RPB. The data reported here include neural responses from at least two monkeys within every area [excepting area CM, where results were similar to previously reported values (20, 27, 28)]. Results were similar across monkeys, and yield and latencies per monkey are listed in Tables S1–S3. For illustrative purposes, an example spike raster, peristimulus time histogram, and response onset latency values for a click response in A1 are included in Fig. 3. As an additional control, latencies were also calculated by four other measures, yielding similar results (Tables S4–S6).

To determine if latencies shift along the core-belt-parabelt hierarchy and caudo-rostral axis, we used a two-factor statistical design (3 × 3 ANOVA). The first factor was regional level where the first level was core, the second level was belt, and the third level was parabelt. The second factor was caudo-rostral position where the first level was most caudal at CM/CL, the second level was intermediate at MM/A1/ML/CPB, and the third level was the most rostral area in the analysis, RM/R/AL/RPB. Note that no core region corresponds to the caudo-rostral level of belt CM and CL. To be conservative in the statistical analysis, CPB was put in the second caudo-rostral level, with A1, MM, and ML. Before selecting these groupings, we additionally confirmed that results in the medial and lateral belt subregions did not differ using a separate planned ANOVA (2 × 3 subregion × caudo-rostral level) and could therefore be combined. This confirmation was done separately for each stimulus and comparison (results below).

Click Latencies. Fig. 4*A* shows a boxplot of the response onset latencies for clicks across the three regions and 10 areas. Here, boxplots are used for visualization as a more complete description of the latency distributions than simple means and SEs (which are reported in Table 1). The latency data show two clear trends

Table 1. Response latency of each area for click, noise and tone stimuli

Stimuli	A1	R	CM	MM	RM	CL	ML	AL	CPB	RPB
Click										
Median	14	20	10	18	35	13.5	20	27.5	25	25
Mean	17.7	26.2	13.9	22.8	33.7	16.8	24.9	31.6	25.7	31.1
SE	0.7	2.0	1.8	1.8	4.0	2.3	2.1	2.9	2.5	3.0
Resp/total	283/536	81/282	30/64	69/158	18/59	30/55	56/155	40/114	33/76	47/157
Noise										
Median	18	28	16	24	33	20	31	28	25.5	25
Mean	22.2	31.3	16.7	27.6	35.8	23.0	35.7	33.3	31.1	29.3
SE	1.0	1.5	2.9	1.9	2.8	2.5	2.4	2.0	3.0	1.8
Resp/total	210/301	120/256	9/9	79/169	30/66	37/58	73/130	80/124	44/83	75/139
Tone										
Median	26	32.5	17.5	26	34	19.5	30	32	27.5	37
Mean	27.9	35.3	22.3	28.5	40.3	24.0	35.0	33.8	31.8	40.2
SE	1.0	1.5	3.8	2.2	5.5	3.5	2.3	2.2	3.6	2.9
Resp/total	175/551	88/299	14/49	35/148	10/46	16/47	33/129	38/108	16/67	29/139

Median, mean, SEM, and number of units responsive/total number recorded are displayed. Latencies are in units of milliseconds.

across areas. First, consistent with anatomical predictions, latencies increase with increasing hierarchical region. For example, latencies in core A1 are faster than belt MM latencies, which are approximately equal to those in belt ML, which in turn are faster than those in parabelt CPB. Second, latencies increase with increasing rostral level. Within a caudo-rostral level, latencies from medial and lateral belt areas are not different from each other. These results were confirmed by a two factor 3×3 region $\times$ caudo-rostral level ANOVA (main effect of region, $P < 0.05$; main effect of caudo-rostral level, $P < 0.05$). A separate planned ANOVA (2×3 subregion $\times$ caudo-rostral level) found no significant differences between the medial belt and lateral belt subregions (subregion $P > 0.05$). In addition, note that the caudal-most belt latencies are as fast or faster latencies than those from the caudal core (A1).

Noise Latencies. Fig. 4*B* shows a boxplot of the response onset latencies for broadband noise across the three regions and 10 areas. As with the clicks, neural latencies were found to increase with hierarchical region and rostral level (ANOVA; region $P < 0.05$; caudo-rostral level $P < 0.05$). Latencies from the medial and lateral belt subregions did not differ (subregion $P > 0.05$).

Tone Latencies. Fig. 4*C* shows a boxplot of the response onset latencies for pure tones across the three regions and 10 areas. Again, similar to the clicks and noise, latencies from the medial and lateral belt subregions did not differ (subregion $P > 0.05$). Tone latencies were not found to increase significantly with increasing hierarchical level, although a trend in this direction was evident (region $P > 0.05$). However, consistent with the results from latencies to click and noise stimuli, latencies did increase significantly with increasing rostral level (caudo-rostral level $P < 0.05$).

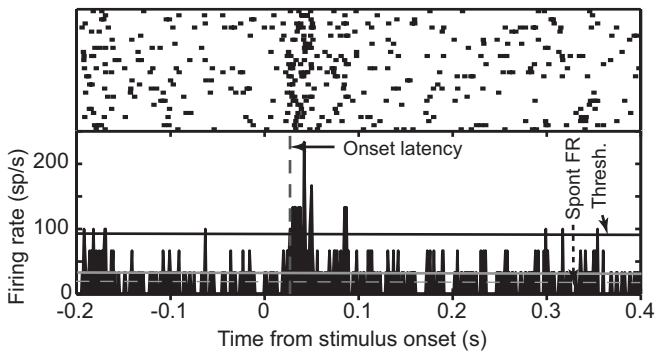

Fig. 3. Example raster, PSTH, and response onset latency values for a click response. Raster, (*Upper*) where each trial is a row. (*Lower*) PSTH with time on the *x* axis and firing rate on the *y* axis. Horizontal gray dashed line is spontaneous firing rate; black line is threshold for Gaussian SD method. Latency is shown by a dotted vertical line.

Discussion

In a survey of 10 areas across three regions of the primate auditory cortex, we find two factors that influence neural onset latencies. First, latencies tend to increase at higher regional levels in the cortical hierarchy, consistent with predictions arising from cortical connectivity. Second, we find that latencies also increase along the caudal-to-rostral axis across areas within the same regional level. This tendency is even more prominent than the effect of regional level, and does not follow immediately as an expected consequence of known cortical connectivity. Previous work has suggested that the caudal aspect of auditory cortex feeds into a "dorsal stream" of auditory processing, and the rostral auditory cortex provides the input to a proposed auditory "ventral stream" (e.g., refs. 8 and 9). Considered within this framework, our present results suggest that the dorsal auditory stream enjoys a timing advantage over the ventral auditory stream.

Differences in species, stimuli, and anesthetic state—all factors known to affect absolute neural latencies—have previously made direct comparisons between latency measures across studies difficult. For example, primate A1 latency estimates range from 10 to 40 ms across studies (19, 20, 23, 25–30). Our present results are consistent with patterns of latency differences across areas (19–22, 26, 29, 31), suggesting possible core-belt-parabelt and caudo-rostral differences, but lack of studies with multiple areas and a lack of physiological descriptions of parabelt CPB and RPB limited conclusions. These results confirm and extend these studies and additionally have the advantage of measuring neural latencies across a large extent of the auditory cortex in the same animal, including the parabelt, using multiple stimuli.

In these data, neural latencies tend to increase at higher hierarchical levels (core-belt-parabelt). Previous studies have shown that neurons in belt areas adjacent to A1 have later responses (19, 23, 27; but see ref. 22), but reports of parabelt latencies are absent in the literature to date. Neural latencies also increase along the caudo-rostral axis within the same hierachical level. This finding is consistent with previous measurements of neural latencies from the core and medial belt (22, 23, 25, 26).

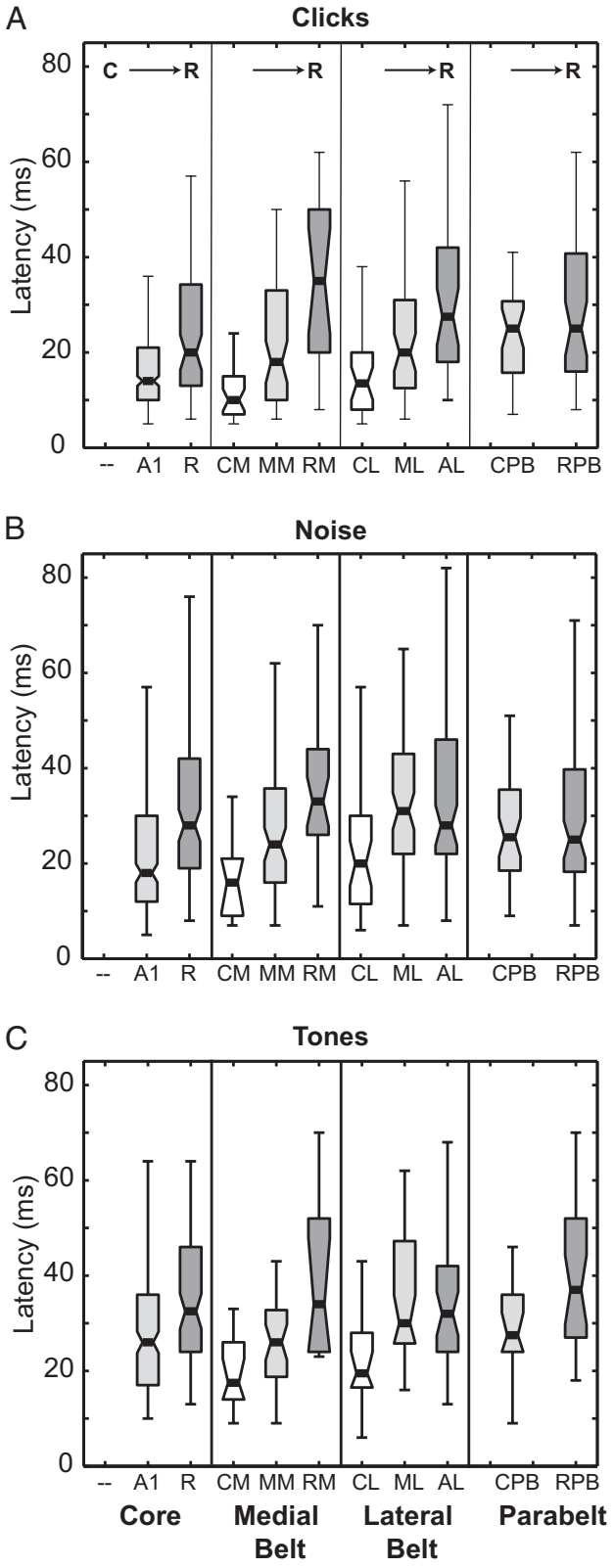

Fig. 4. Boxplots of unit latencies per area. (*A*) Click latencies. (*B*) Noise latencies. (*C*) Tone latencies at BF + neighboring frequencies. For each plot, each region is separated by a vertical line (belt is separated into medial and lateral subregions), and areas within each region are arranged in a caudal-to-rostral direction. The color/shade of the boxplot indicates relative caudo-rostral level. The box denotes the upper quartile, median, and lower quartile of the distribution. Whiskers denote the extent of the rest of the data. Notches indicate an estimate of the uncertainty about the median. If notches do not overlap, the medians differ at the α-level of $P < 0.05$. Because CPB receives projections from belt areas at both the first and second caudo-rostral level, for visualization purposes it is placed in between the tick marks.

Although responses to the different stimuli (click, noise, tone) differ in their absolute latencies, we find broadly consistent patterns of relative latency differences across stimulus types, despite differences in envelope, duration, and bandwidth. This finding suggests that our results are likely to be representative of the timing of information flow for the majority of ethologically relevant stimuli. Given the proposed differences in the thalamocortical pathways for tone compared with broadband sound propagation (e.g., ref. 21), these similarities may be surprising. However, at suprathreshold levels as in this study, narrowly tuned neurons are often responsive to a broad range of frequencies. These suprathreshold stimuli may therefore activate similar sequences of pathways.

Note that click stimulation provides unique advantages in the assay of latencies across areas. First, it is a broadband stimulus to which many neurons are highly responsive. Second, because it has a sharp and quick onset and offset, measurements of long latency responses are not complicated by responses to stimulus offsets. Click latencies are thus likely to represent an upper bound on the rate of information transfer across the auditory cortex. Similar reasoning has led to the use of brief, broadband stimuli in studies investigating response latencies across the visual system (5, 6), and in the auditory potentials in cortex (28, 32). Despite this finding, for clicks and all other stimuli, the distributions of unit latencies within a given area are quite broad. This result is most likely because of known differences in latency within the lamina and even across cell classes (33-37). Future studies examining and comparing latencies in identified lamina and cell class across areas would be useful to extend the comparison.

In addition to the broad agreement with electrophysiological predictions of a core-belt-parabelt hierarchy, these results additionally fit with anatomical predictions made for cortical activation timing across regions. Corticocortical connectivity patterns lead to clear predictions for the relative latencies of core, belt, and parabelt activity, with longer latencies expected at higher hierarchical levels. In addition, anatomical connection patterns also suggest that medial and lateral belt subregions belong to the same regional level (18). We find minimal differences between these regions in the timing of cortical activation of the areas, supportive of this model. General patterns of latencies between regions are further consistent with chemoarchitectural gradients observed across regional levels (12, 18, 38). Cytochrome oxidase expression, a marker of metabolic activity often seen in fast cortices and pathways, is most dense in the core and least dense in the parabelt. Our present physiological observations between regions are fully consistent with predictions made from anatomical connectivity and chemoarchitectural gradients.

An interesting exception to this general core-belt-parabelt hierarchy are the extremely fast latencies seen in caudal belt CM and CL, relative to latencies in neighboring core A1. Some caution may be warranted in the interpretation of results from area CM, as it had a low number of units sampled, coming from only one monkey. However, our results in this area are consistent with absolute latency values reported in previous studies, and more importantly, are consistent with previous reports of CM latencies as fast or faster than A1 (19, 20, 30). Closer examination of the anatomical topography of thalamic inputs may suggest a resolution to this conundrum. The caudal belt, particularly CM and CL, receive projections from an anterior portion of the MGd, the MGad. This region has not been well characterized in primates, but a possibly corresponding structure in the MGB of cats has been found to exhibit fast latencies comparable to the

MGv (39–41). Projections from the MGad to both the medial and lateral belt decrease in strength as one progresses rostrally, and are almost absent at the level of RM (42, 43), which is then characterized by a dense projection from the MGpd. Thus, it is possible that the shortest latencies in the caudal-most portion of belt are driven by fast direct thalamic input from MGad. To confirm this hypothesis, the connections and response properties of the divisions of the MGC must be better characterized.

Another possible exception is that for clicks and noise, latencies in AL appear to be as short or shorter than RPB. Although the median latencies of RPB responses are indeed somewhat shorter than those of AL in for these stimuli, these differences are not statistically significant (t test $P > 0.05$). An alternative, and likely interpretation is that the rostral tip of RPB was inaccessible with our grids, so the distribution of RPB latencies does not reflect the longest latencies from the rostral tip, and it is likely that RPB latencies are actually longer than reported here.

A second result from these data does not immediately fit with known anatomical connections: within the same region, rostral latencies are slower than caudal latencies. Although anatomical connections do not immediately account for these caudo-rostral latency trends, the chemoarchitecture of the caudal areas suggests they may be very fast. Caudal areas are notably dense in cytochrome oxidase relative to rostral areas. Additionally, cortico-cortical connectivity of some areas is suggestive of feedforward activity (connections to layer 4) in the rostral direction (16, 17). However, this finding has not been demonstrated conclusively for all areas (18). Although this result is not immediately predicted by known connectivity, quantitative studies of laminar and thalamo-cortical connectivity would help to explain this intriguing trend, and possibly suggest potential specializations along this axis.

Although there are clear regional and caudo-rostral trends in the measured neural latencies, there is also substantial overlap in their distributions, suggestive of some degree of parallelism in the flow of information. Given the numerous parallel pathways from the MGC, evidence for parallel processing is perhaps unsurprising. For example, neural responses in the belt and parabelt, at differing regional levels, are driven by a mixture of inputs from distinct, serial, cortical pathways and multiple overlapping, parallel, thalamic sources. Because of the ongoing temporal nature of sound, auditory stimuli must be processed very rapidly. A system that is wired to process information across many streams simultaneously is likely better suited for fast processing than a strictly serial hierarchy. We would argue that such massive parallelism is a hallmark of the auditory system, imposed by timing constraints on the processing of auditory stimuli.

Taken together, these results suggest commonalities across cortical sensory systems, in particular to the visual system. The visual system is commonly divided into dorsal and ventral streams, often interpreted as primarily subserving location and identity, respectively (although there is overlap). In the visual system, the dorsal stream has faster neural response latencies and exhibits a significant timing advantage over the ventral stream (5, 6). Such a dorsal stream timing advantage is thought to potentially confer the evolutionary advantage of supporting rapid processing of where a stimulus is for action selection (e.g., under threat). Based on the topography of prefrontal cortical projections from the auditory cortex, it has been suggested that auditory processing is also divided into dorsal and ventral streams (e.g., refs. 7–9). Accumulating evidence from this study and others suggest that caudal auditory cortical areas feeding into the auditory dorsal stream have faster response latencies than cortical areas feeding into the auditory ventral stream. This finding suggests there may exist a common supramodal design principle, where the dorsal stream has a general timing advantage over the ventral stream in cortical sensory processing.

Methods

Animal Subjects. Three adult macaque monkeys PJ, SP, and DY were involved in neural recordings [PJ: a female bonnet macaque (*Macaca radiata*) 5.0 kg; SP: amale bonnet macaque 10.0 kg; and DY: afemale rhesus macaque (*Macaca mulatta*) 7.0 kg]. Animals were housed in an Association for Assessment and Accreditation of Laboratory Animal Care-accredited facility under the supervision of laboratory and veterinary staff. All animal care and experimental procedures were in accordance with the National Institutes of Health *Guide for the Care and Use of Laboratory Animals*, under a protocol approved by the Vanderbilt Institutional Animal Care and Use Committee. For consistency, data were collected exclusively from the left hemisphere of each monkey. Further details of surgical procedures can be found in *Supporting Information*. At the end of the experiment, location of electrode tracks were identified. Further details of the histology and identification of cortical areas can be found in *Supporting Information*.

Stimulus Generation and Neurophysiological Acquisition. ***Stimulus generation and delivery.*** Recording sessions were conducted in a double-walled sound-attenuated chamber (Acoustic Systems). Acoustic stimuli were generated by Tucker-Davis Technologies System II hardware and software (SigGen), controlled by a custom software interface between the stimulus generation and acquisition setups. Stimuli were delivered using Beyer DT911 insert earphones (range 0.1–25.0 kHz), coupled to custom earmolds in both ears. These earmolds were made individually for each monkey by constructing a silicon mold of the concha and first few millimeters of the ear canal of each ear to completely seal the ear canal. A stainless-steel tube (inner diameter ~1 mm) passed through the ear mold to protrude 2–3 mm into the ear canal. The transducer tube interfaced to the mold tube to form a sealed system. Stimuli were calibrated for intensity using a 0.25-inch microphone (Model 7017; ACO Pacific), pistonphone (Bruel and Kjaer type 4220) and custom software (Tucker-Davis Technologies, SigCal). Amplitude corrections were saved in a data file and applied to each stimulus to preequalize the response of each earphone independently.

Stimuli. All stimuli were delivered diotically with a jittered interonset interval of ~1,000 ms, randomly interleaved with other stimulus types in the battery (e.g., tones, noise, sinusoidally amplitude-modulated noise). Diphasic clicks were 0.25 ms in duration, calibrated to 60 dB SPL, and presented 30 times. Gaussian white noise was 200 ms in duration (5 ms cosine^2 onset/offset ramp), calibrated to 60 dB SPL, and presented 30 times. Pure tones were 50 ms in duration (5 ms cosine^2 onset/offset ramp) and ranged from 0.3 to 21.0 kHz in one-third octave steps. The tone stimuli were shorter to allow for a more extensive battery of four intensities (15, 30, 45, 60 dB SPL), so as to efficiently estimate the frequency response area. Each frequency-intensity combination was presented in random order 10 times. To be comparable to the levels of the click and noise stimuli, tone latencies reported are from the 60-dB intensity (details below).

Electrophysiological recording. Electrode penetrations were made through a recording grid 15-mm wide with 1-mm spacing that fit over the implanted chamber (Crist Instruments). This process ensured a replicable and roughly perpendicular trajectory through most parts of the superior temporal plane corresponding to the caudal two-thirds of the auditory cortex. After a local anesthetic (0.13% bupivacaine and 0.50% lidocaine in sterile saline) was topically applied and then removed, a sharpened stainless-steel guide tube was inserted to puncture the dura. The use of a guide tube also ensured that the penetration ran parallel to the recording chamber. One or two tungsten microelectrodes (2–4 MΩ; FHC), aligned mediolaterally, were advanced through the guide tube through parietal cortex and into auditory cortex using manual microdrives (Narishige).

From the first auditory responses until the end of the auditory-responsive cortex, all isolated neurons, irrespective of apparent responsiveness, were tested with all or most of the stimulus battery, so as to avoid sampling bias. Between isolations the microdrives were moved at least 200 μm to avoid resampling units. For most runs, we recorded through all layers until the white matter was reached. We assigned a relative cortical depth to each penetration by normalizing the recording depth with respect to the first auditory responses, presumably from the first layer or two of auditory cortex. Although unequivocal laminar depths cannot be established, it is likely that the majority of recorded neuronal responses come from the middle and upper layers, consistent with the cytoarchitecture of the auditory cortex (11). During recording sessions the monkey sat passively and was continuously monitored for alertness via closed-circuit television.

Multichannel spike and local field potential recordings were acquired with a 64-channel system that controls amplification, filtering, and related parameters (Many Neuron Acquisition Processor; Plexon). Both signals were referenced to ground. Spike signals were amplified (100×), filtered (150–8,800 Hz), and

digitized at 40 kHz. The signal was further DC-offset–corrected with a low-cut filter (0.7 Hz). Spikes were initially sorted online for all channels using real-time window discrimination. Digitized waveforms and timestamps of stimulus events were also saved for final offline analysis and final sorting (Plexon offline sorter), and graded according to isolation quality (single or multiunits). Single and multiunits were analyzed separately. Because the patterns of results were similar, data from both single and multiunits were included in the results. To ensure timing precision, the Plexon acquisition software interfaced with the stimulus delivery system (Tucker-Davis Technologies) and both systems were controlled by custom software (SGPlay; Tucker-Davis Technologies, provided by Peter Yang, independent contractor, Nashville, TN).

Neurophysiological data analysis. All analyses described below were done using in-house Matlab scripts (MathWorks), confirmed when possible by Neuroexplorer v3.021 (Nex Technologies). Spike times were binned at 1 ms to maintain the precision of latency measures. The method to calculate response onset latency of each neuron was calculated similarly for all stimuli (clicks, noise, and tones), using the Gaussian SD algorithm, used in other studies of awake auditory cortex (e.g., refs. 22, 26, 27). This algorithm is based on the averaged neural response in the form of a peristimulus time histogram (PSTH). The neural latency was the first bin after stimulus presentation to cross a response threshold and remain there for a minimum number of bins (here, three bins). The algorithm defined a response threshold as 3 Gaussian SDs of the spontaneous rate above the mean spontaneous firing rate. To aid in precision in spike timing, no smoothing functions were used. Spontaneous firing rate measures were derived from the period 200–0 ms before stimulus onset. To ensure results were consistent across different latency measures, four other measures were used (*SI Text*). For tones, latencies were derived from the group of three frequencies that produced the best response (BF) + the neighboring frequencies [edge frequencies had only one neighbor and were normalized appropriately (similar to ref. 19)]. Combining responses from three neighboring frequencies reduced noise in the determination of the BF, and had the additional benefit of normalizing the number of stimulus presentations to 30 for all three kinds of stimuli in this study. To ensure reliability, the BF was derived by analyzing firing rates in two different windows: (*i*) 10–100 ms poststimulus onset and (*ii*) from response onset latency to 100 ms after onset latency. Regardless of the analysis window, tuning was similar; these were confirmed by examination of the full frequency response area and additionally showed that at 60 dB, no neurons exhibited inhibition at frequencies directly neighboring the BF.

ACKNOWLEDGMENTS. The authors thank Warren Lambert for statistical consultation. This research was supported by National Institutes of Health/National Institute on Deafness and Other Communication Disorders Grant R01 DC-04318 (to T.A.H.) and National Institute of Child Health and Human Development Grant P30 HD15052 (to the Vanderbilt Kennedy Center).

1. Kaas JH (2012) The evolution of neocortex in primates. *Prog Brain Res* 195:91–102.
2. Kaas JH (1997) Topographic maps are fundamental to sensory processing. *Brain Res Bull* 44(2):107–112.
3. Ungerleider L, Mishkin M (1982) Two cortical visual systems. *Analysis of Visual Behavior*, eds Ingram DJ, Goodale MA, Mansfield RJW (MIT Press, Cambridge, MA), pp 549–586.
4. Ungerleider LG, Galkin TW, Mishkin M (1983) Visuotopic organization of projections from striate cortex to inferior and lateral pulvinar in rhesus monkey. *J Comp Neurol* 217(2):137–157.
5. Schroeder CE, Mehta AD, Givre SJ (1998) A spatiotemporal profile of visual system activation revealed by current source density analysis in the awake macaque. *Cereb Cortex* 8(7):575–592.
6. Schmolesky MT, et al. (1998) Signal timing across the macaque visual system. *J Neurophysiol* 79(6):3272–3278.
7. Romanski LM, Bates JF, Goldman-Rakic PS (1999) Auditory belt and parabelt projections to the prefrontal cortex in the rhesus monkey. *J Comp Neurol* 403(2):141–157.
8. Romanski LM, et al. (1999) Dual streams of auditory afferents target multiple domains in the primate prefrontal cortex. *Nat Neurosci* 2(12):1131–1136.
9. Rauschecker JP, Tian B (2000) Mechanisms and streams for processing of "what" and "where" in auditory cortex. *Proc Natl Acad Sci USA* 97(22):11800–11806.
10. Kaas JH, Hackett TA (2000) Subdivisions of auditory cortex and processing streams in primates. *Proc Natl Acad Sci USA* 97(22):11793–11799.
11. Hackett TA (2011) Information flow in the auditory cortical network. *Hear Res* 271(1–2):133–146.
12. Hackett TA, Stepniewska I, Kaas JH (1998) Subdivisions of auditory cortex and ipsilateral cortical connections of the parabelt auditory cortex in macaque monkeys. *J Comp Neurol* 394(4):475–495.
13. Molinari M, et al. (1995) Auditory thalamocortical pathways defined in monkeys by calcium-binding protein immunoreactivity. *J Comp Neurol* 362(2):171–194.
14. Burton H, Jones EG (1976) The posterior thalamic region and its cortical projection in New World and Old World monkeys. *J Comp Neurol* 168(2):249–301.
15. Jones EG, Burton H (1976) Areal differences in the laminar distribution of thalamic afferents in cortical fields of the insular, parietal and temporal regions of primates. *J Comp Neurol* 168(2):197–247.
16. Fitzpatrick KA, Imig TJ (1980) Auditory cortico-cortical connections in the owl monkey. *J Comp Neurol* 192(3):589–610.
17. Galaburda AM, Pandya DN (1983) The intrinsic architectonic and connectional organization of the superior temporal region of the rhesus monkey. *J Comp Neurol* 221(2):169–184.
18. de la Mothe LA, Blumell S, Kajikawa Y, Hackett TA (2006) Cortical connections of the auditory cortex in marmoset monkeys: Core and medial belt regions. *J Comp Neurol* 496(1):27–71.
19. Recanzone GH (2000) Response profiles of auditory cortical neurons to tones and noise in behaving macaque monkeys. *Hear Res* 150(1-2):104–118.
20. Kajikawa Y, de la Mothe L, Blumell S, Hackett TA (2005) A comparison of neuron response properties in areas A1 and CM of the marmoset monkey auditory cortex: Tones and broadband noise. *J Neurophysiol* 93(1):22–34.
21. Lakatos P, et al. (2005) Timing of pure tone and noise-evoked responses in macaque auditory cortex. *Neuroreport* 16(9):933–937.
22. Kusmierek P, Rauschecker JP (2009) Functional specialization of medial auditory belt cortex in the alert rhesus monkey. *J Neurophysiol* 102(3):1606–1622.
23. Bieser A, Müller-Preuss P (1996) Auditory responsive cortex in the squirrel monkey: Neural responses to amplitude-modulated sounds. *Exp Brain Res* 108(2):273–284.
24. Scott BH, Malone BJ, Semple MN (2011) Transformation of temporal processing across auditory cortex of awake macaques. *J Neurophysiol* 105(2):712–730.
25. Kikuchi Y, Horwitz B, Mishkin M (2010) Hierarchical auditory processing directed rostrally along the monkey's supratemporal plane. *J Neurosci* 30(39):13021–13030.
26. Bendor D, Wang X (2008) Neural response properties of primary, rostral, and rostrotemporal core fields in the auditory cortex of marmoset monkeys. *J Neurophysiol* 100(2):888–906.
27. Vaadia E, Gottlieb Y, Abeles M (1982) Single-unit activity related to sensorimotor association in auditory cortex of a monkey. *J Neurophysiol* 48(5):1201–1213.
28. Steinschneider M, et al. (1992) Cellular generators of the cortical auditory evoked potential initial component. *Electroencephalogr Clin Neurophysiol* 84(2):196–200.
29. Cheung SW, Bedenbaugh PH, Nagarajan SS, Schreiner CE (2001) Functional organization of squirrel monkey primary auditory cortex: Responses to pure tones. *J Neurophysiol* 85(4):1732–1749.
30. Oshurkova E, Scheich H, Brosch M (2008) Click train encoding in primary and non-primary auditory cortex of anesthetized macaque monkeys. *Neuroscience* 153(4):1289–1299.
31. Philibert B, et al. (2005) Functional organization and hemispheric comparison of primary auditory cortex in the common marmoset (*Callithrix jacchus*). *J Comp Neurol* 487(4):391–406.
32. Inui K, Okamoto H, Miki K, Gunji A, Kakigi R (2006) Serial and parallel processing in the human auditory cortex: A magnetoencephalographic study. *Cereb Cortex* 16(1):18–30.
33. Sakata S, Harris KD (2009) Laminar structure of spontaneous and sensory-evoked population activity in auditory cortex. *Neuron* 64(3):404–418.
34. Wallace MN, Palmer AR (2008) Laminar differences in the response properties of cells in the primary auditory cortex. *Exp Brain Res* 184(2):179–191.
35. Sugimoto S, Sakurada M, Horikawa J, Taniguchi I (1997) The columnar and layer-specific response properties of neurons in the primary auditory cortex of Mongolian gerbils. *Hear Res* 112(1-2):175–185.
36. Atencio CA, Schreiner CE (2008) Spectrotemporal processing differences between auditory cortical fast-spiking and regular-spiking neurons. *J Neurosci* 28(15):3897–3910.
37. Atencio CA, Schreiner CE (2010) Columnar connectivity and laminar processing in cat primary auditory cortex. *Plos One* 5(3):e9521.
38. Jones EG, Dell'Anna ME, Molinari M, Rausell E, Hashikawa T (1995) Subdivisions of macaque monkey auditory cortex revealed by calcium-binding protein immunoreactivity. *J Comp Neurol* 362(2):153–170.
39. Imig TJ, Morel A (1984) Topographic and cytoarchitectonic organization of thalamic neurons related to their targets in low-, middle-, and high-frequency representations in cat auditory cortex. *J Comp Neurol* 227(4):511–539.
40. Imig TJ, Morel A (1985) Tonotopic organization in lateral part of posterior group of thalamic nuclei in the cat. *J Neurophysiol* 53(3):836–851.
41. Imig TJ, Morel A (1985) Tonotopic organization in ventral nucleus of medial geniculate body in the cat. *J Neurophysiol* 53(1):309–340.
42. de la Mothe LA, Blumell S, Kajikawa Y, Hackett TA (2006) Thalamic connections of the auditory cortex in marmoset monkeys: Core and medial belt regions. *J Comp Neurol* 496(1):72–96.
43. Hackett TA, et al. (2007) Multisensory convergence in auditory cortex, II. Thalamocortical connections of the caudal superior temporal plane. *J Comp Neurol* 502(6):924–952.
44. Wong-Riley M (1979) Changes in the visual system of monocularly sutured or enucleated cats demonstrable with cytochrome oxidase histochemistry. *Brain Res* 171(1):11–28.
45. Geneser-Jensen FA, Blackstad TW (1971) Distribution of acetyl cholinesterase in the hippocampal region of the guinea pig. I. Entorhinal area, parasubiculum, and presubiculum. *Z Zellforsch Mikrosk Anat* 114(4):460–481.
46. Gallyas F (1979) Silver staining of myelin by means of physical development. *Neurol Res* 1(2):203–209.
47. Hackett TA, Stepniewska I, Kaas JH (1998) Thalamocortical connections of the parabelt auditory cortex in macaque monkeys. *J Comp Neurol* 400(2):271–286.
48. Hackett TA, Preuss TM, Kaas JH (2001) Architectonic identification of the core region in auditory cortex of macaques, chimpanzees, and humans. *J Comp Neurol* 441(3):197–222.
49. Hackett TA, de la Mothe LA (2009) Regional and laminar distribution of the vesicular glutamate transporter, VGluT2, in the macaque monkey auditory cortex. *J Chem Neuroanat* 38(2):106–116.